

PHYSICAL REVIEW LETTERS

VOLUME 17

19 SEPTEMBER 1966

NUMBER 12

TEST OF THE THEORY OF STARK BROADENING OF H_{β} *

J. B. Gerardo and R. A. Hill
Sandia Laboratory, Albuquerque, New Mexico
(Received 15 August 1966)

Plasma electron densities inferred from the half-intensity width of H_{β} are shown to agree to within $\pm 1.5\%$ with those measured by laser interferometry.

The development of the theory of Stark broadening, i.e., broadening caused by the electric microfields of the free charged particles in a plasma, has provided an important tool for the diagnostics of high-density gaseous plasmas.¹⁻³ It has been shown that the experimental profiles for the first four Balmer lines agree with the theoretical profiles to within the predicted accuracy of the theory.^{4,5} Furthermore, electron densities which are inferred from the half-intensity width of H_{β} have been shown to agree to within $\pm 6\%$ with the values obtained with a Mach-Zehnder interferometer.⁶ The inability to make a more accurate test of the theoretical profiles has been due in part to difficulties in measuring accurately the electron density by some independent means, difficulties in obtaining very uniform plasmas, and difficulties in recording time-resolved line profiles. In the following we discuss recent results which show that the electron density inferred from the half-intensity width of H_{β} agrees to within $\pm 1.5\%$ with the value obtained by an optical interferometric technique. This accuracy was obtained by measuring the electron density with a multiple-pass laser interferometer, by using a long, uniform plasma column in order to minimize the effects of the cold boundary layer at the tube walls, and by recording the line profiles with a rapid-scan spectrometer.

The experimental apparatus is illustrated in Fig. 1. Two laser interferometers,^{7,8} operating at wavelengths of $\lambda_1 = 1.1523\mu$ and $\lambda_2 = 0.6328\mu$, respectively, were used in order to eliminate the effect of changes in optical path length due to changes in neutral atom concentration and the possible effect of excited atoms. For the frequencies involved in this experiment, the polarizability of neutral hydrogen in both ground and excited states is nearly independent of wavelength. Thus, to an estimated accuracy of better than 0.1% , the electron density is given by

$$N_e = \frac{1.247 \times 10^{13}}{d_p (\lambda_1^2 - \lambda_2^2)} \left[\frac{\chi_1 \lambda_1}{S_1} - \frac{\chi_2 \lambda_2}{S_2} \right], \quad (1)$$

where d_p is the plasma length, χ represents the number of observed fringes, and S represents the number of passes made by a laser

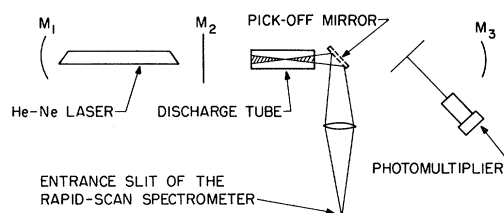


FIG. 1. A schematic of the multiple-pass laser interferometer. The pick-off mirror is moved into position only when spectra are being recorded.

beam through the plasma. Because $\lambda_1/S_1 \gg \lambda_2/S_2$, the accuracy of the electron-density measurement is determined predominantly by the accuracy of the fringe-shift measurement χ_1 , which is estimated to be $\pm 1/15$ of a fringe. Thus, with a nominal fringe shift of 5 full fringes, the accuracy of the measurement is $\pm 1.3\%$.

The plasma was formed in a discharge tube (14.9 cm long and 3.0 cm inside diameter) which was fitted with narrow brass-ring electrodes. The plasma was produced by discharging a critically damped 2- μ F capacitor charged to 25 kV into pure hydrogen gas at a pressure of 1.0 Torr. 90% of the time, consecutive discharges reproduced the fringe pattern of the 1.1523- μ laser interferometer to within the accuracy with which the fringes could be measured. It was also determined, by means of the interferometer, that in the early afterglow, the electron density was uniform over the central 2.6-cm-diam portion of the cross section to within the accuracy of the measurement ($\pm 1.3\%$). At 0.2 cm from the sidewall, the electron density fell very rapidly, and this steep gradient prevented accurate density measurements in this region. The thickness of the boundary layer at the tube windows was assumed to be identical to that at the sidewalls. Hence, an effective plasma length of 14.7 cm was used in Eq. (1). Typical interferometer recordings are illustrated in Fig. 2(a) and 2(b).

The spectroscopic data were obtained with an $f/5.3$ rapid-scan spectrometer operating at a spectral scan speed of $83.65 \pm 0.05 \text{ \AA}/\mu\text{sec}$.⁹ The effective spectral slit width was 0.74 \AA . A Tektronix type-551 dual-beam oscilloscope was used to record simultaneously both the spectra and timing marks from a 5-Mc/sec crystal-controlled pulser which were used for sweep speed calibration. The H_β line profiles were recorded at a sweep rate of 0.2 $\mu\text{sec}/\text{division}$ (div) giving a spectral dispersion of 16.73 $\text{\AA}/\text{div}$. The radiation from the plasma was focused on the entrance slit of the spectrometer as illustrated in Fig. 1. The maximum diameter of the acceptance cone inside the plasma tube was 1.4 cm which is sufficiently small so as to exclude radiation from the walls of the tube. Radiation emitted from the thin boundary layer at the end windows was neglected, since this radiation was estimated to contribute less than 1% to the total. A typical H_β line profile is shown in Fig. 2(c).

The interferometric and spectroscopic data

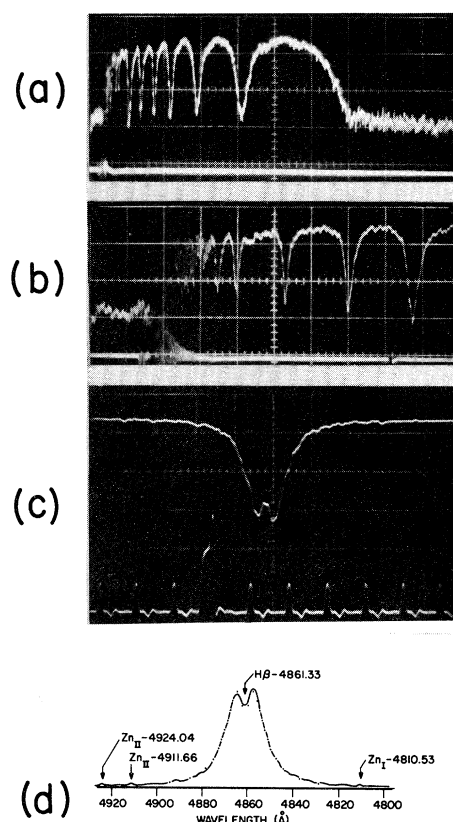


FIG. 2. Typical interferometer and spectrometer recordings. (a) $\lambda = 1.1523 \mu$ at 10 $\mu\text{sec}/\text{div}$. (b) $\lambda = 1.1523 \mu$ at 2 $\mu\text{sec}/\text{div}$. (c) An H_β line profile at 0.2 $\mu\text{sec}/\text{div}$. The timing marks are from a 5-Mc/sec crystal-controlled pulser. The timing pulse, recorded on the lower traces, is derived from the firing of the discharge tube. (d) Comparison of an observed H_β profile [Fig. 2(c)] with its theoretical profile (dots). The narrow band at the bottom is the continuum intensity. $T = 2 \times 10^4 \text{ }^\circ\text{K}$. $N_e = 2.78 \times 10^{16} \text{ cm}^{-3}$.

were recorded alternately so that good statistics were obtained on the reproducibility. The two measurements were correlated in time by recording a timing pulse which was derived from the initiation of the discharge. The interferometric data have been plotted in Fig. 3 at each of the times for which an H_β profile was recorded. The H_β profiles were analyzed by averaging the heights of the two peaks, and then measuring the half-intensity and tenth-intensity widths. The position of the base line was determined by recording several line profiles at increased sensitivity, so that accurate H_β -to-continuum ratios could be calculated. These ratios gave an electron temperature of $2.1 \pm 0.2 \text{ eV}$.³ Tables of electron density as a function of the H_β half-intensity width¹⁰ and

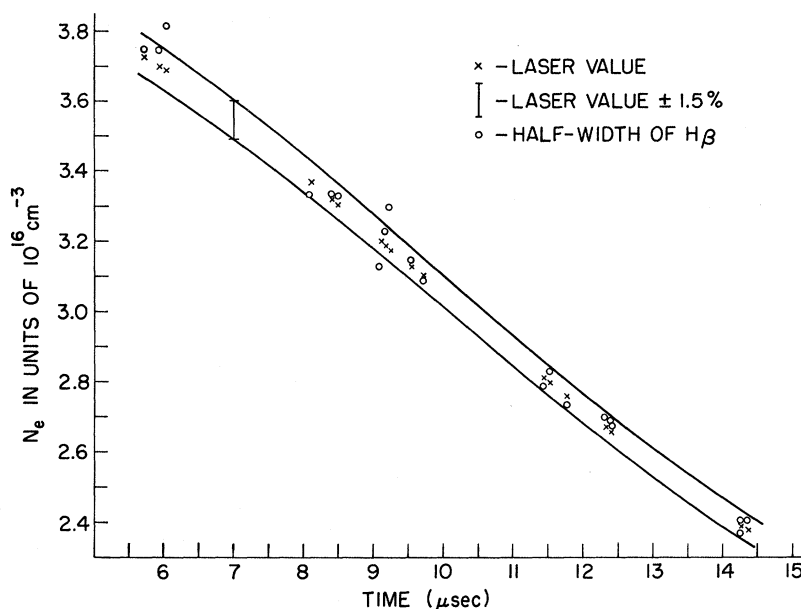


FIG. 3. Comparison of the values of electron density from the laser interferometer and half-intensity width of H_β . The discharge was initiated at $t = 0$, and current duration was approximately $2 \mu\text{sec}$.

of the H_β tenth-intensity width were used to obtain values for the electron density, which were in excellent self-agreement. These values for the electron density are also plotted in Fig. 3, and all except three points agree to within $\pm 1.5\%$ with the interferometric values. The greater deviation of these three points is attributed to the occasional, slight nonreproducibility of the plasma. The data points in Fig. 3 represent all of the data recorded in a particular experimental run. This experiment has been repeated several times; each time, this very good agreement between the two measuring techniques has been obtained. Because of possible compensating errors, the theoretical profiles may not be quite so accurate as this $\pm 1.5\%$ agreement would indicate. However, detailed estimates of possible compensating errors indicate that less than $\pm 1\%$ additional error would be expected. A comparison of an observed and theoretical profile is shown in Fig. 2(d). The three weak contaminant lines on the recording show that the H_β profile is not measurably shifted in wavelength. The central dip in the recorded profile is not so deep as expected theoretically and on all recorded profiles, the blue peak is somewhat more intense than the red peak. This intensity distribution remains unaltered, whether the scanning direction is from the red to blue or blue to red. However, it must be concluded that

excellent agreement exists between the theoretical and observed profile.

Several H_β profiles were also recorded from the side of the discharge tube. In this manner, it was found that the plasma column was uniform along the length of the tube. However, the densities measured from the half-widths of these "side-on" profiles were some 10% lower than the densities which were measured "end on." Since boundary layer effects contribute a higher percentage of the energy "side on" than "end on," this discrepancy is not surprising. It does indicate the pronounced effect of the narrow boundary layer on the net profile and points out that even very small plasma nonhomogeneities can lead to gross misinterpretation of data.

*This work was supported by the U. S. Atomic Energy Commission.

¹H. R. Griem, A. C. Kolb, and K. Y. Shen, Phys. Rev. **116**, 4 (1959).

²H. R. Griem, A. C. Kolb, and K. Y. Shen, Astrophys. J. **135**, 272 (1962).

³H. R. Griem, *Plasma Spectroscopy* (McGraw-Hill Book Company, Inc., New York, 1964).

⁴H. F. Berg, A. W. Ali, and H. R. Griem, Phys. Rev. **125**, 199 (1962).

⁵W. L. Wiese, D. R. Paquette, and J. E. Solariski, Phys. Rev. **129**, 1225 (1963).

⁶E. A. McLean and S. A. Ramsden, Phys. Rev. **140**, A1122 (1965).

⁷J. B. Gerardo and J. T. Verdeyen, Proc. IEEE 52, 690 (1964).

⁸J. B. Gerardo, J. T. Verdeyen, and M. A. Gusinow, J. Appl. Phys. 36, 2146 (1965).

⁹R. A. Hill and R. D. Fellerhoff, Appl. Opt. 5, 1105 (1966).

¹⁰R. A. Hill, J. Quant. Spectr. Radiative Transfer 4, 857 (1965).

PULSED TRANSMISSION AND RINGING PHENOMENA IN A WARM MAGNETOPLASMA*

F. W. Crawford, R. S. Harp, and T. D. Mantel

Institute for Plasma Research, Stanford University, Stanford, California

(Received 25 July 1966; revised manuscript received 17 August 1966)

This Letter describes studies of the group velocity of a wave packet propagating radially across a plasma immersed in a static axial magnetic field. The experimental results reproduce in the laboratory a ringing effect, previously observed only in the ionosphere, for which an explanation is given in terms of warm magnetoplasma wave theory. Since the phenomena concerned are only predicted by microscopic theory, the close agreement between experiment and such theory for the observations reported provides a powerful check on its validity.

The first aim of this work was to reproduce in the laboratory a phenomenon first observed with the "Alouette" satellite.¹ It was found in the course of experiments with this vehicle that the response of the ionosphere to a pulsed transmitter of variable frequency, ω , showed prolonged ringing effects after the end of the transmitter pulse whenever $\omega = n\omega_c$ ($n = 2, 3, 4, \dots$) or $\omega = (\omega_p^2 + \omega_c^2)^{1/2}$, i.e., at the electron-cyclotron frequency harmonics and at the upper hybrid frequency. An explanation for the results was advanced in terms of cyclotron harmonic waves (CHW).² This mode of propagation can only be derived from microscopic magnetoplasma wave theory which predicts phenomena not appearing in a hydrodynamic treatment.³ Landau damping of longitudinal wave ($\vec{k} \cdot \vec{E}$) propagation with $B = 0$, or along the magnetic field ($k_{\perp} = 0, k_{\parallel} \neq 0$), is one example that has been demonstrated recently experimentally.⁴ Another is CHW propagation, which, for $k_{\parallel} \neq 0, k_{\perp} \neq 0$, is predicted to occur in passbands bounded by $n\omega_c$. These longitudinal waves are subject to collisionless damping unless $k_{\parallel} = 0, k_{\perp} \neq 0$, when the CHW dispersion relation, $\epsilon_{\perp} = 0$, derives directly from the perpendicular component of the warm-plasma relative-permittivity tensor,³

$$\epsilon_{\perp} = 1 - (\omega_p^2 / \omega_c^2) \sum_{n=1}^{\infty} \frac{2 \exp(-\lambda) I_n(\lambda)}{\lambda (\omega / n\omega_c^2 - 1)}. \quad (1)$$

Here ω_p is the electron plasma frequency; $\lambda = (k_{\perp} R)^2$, and $R = [(\kappa T_e / m)^{1/2} / \omega_c]$ is the Larmor radius of a particle with thermal speed.

The validity of Eq. (1) has been supported by (i) admittance measurements.^{2,5} These are obtained by observing the received signal on one of two similar wire probes immersed in the plasma, and oriented parallel to B , when the other is excited. The location of a series of peaks supports qualitatively an admittance viewpoint in which $\epsilon_{\perp} \neq 0$. (ii) Interference observations.⁵ Admittance peaks may be accompanied by a fine structure of smaller peaks due to interference between the direct admittance component and the fields of propagating CHW. The interference pattern can be interpreted to agree well with Eq. (1). (iii) Noise and absorption observations.^{6,7} Peaks observed in emission and absorption are similar to those of (ii). The fine structure has been analyzed very successfully in terms of standing CHW in an inhomogeneous plasma.

The present experiment differs from (i) in that it is quantitative; from (ii) in that it separates the CHW propagation and the direct component; and from (iii) in that plane wave propagation in a homogeneous infinite plasma is studied effectively. The setup is shown in Fig. 1 (inset). Radio-frequency pulses at 800 MHz, ≈ 40 nsec long, are applied to one of two parallel antennas immersed in a substantially uniform plasma region, and are received on the other. The band-pass filter improves the pulse shape, by restricting the bandwidth. The final envelope closely approaches a Gaussian with frequency spread of about $\pm 4\%$. Beyond this the Fourier component amplitudes are down by e or more. Typical signals taken with a graphical recorder connected to the sampling oscilloscope are shown in Fig. 1 for various antenna separations. In each case, the first pulse is due to direct coupling, while the second is the wave packet traveling in the CHW

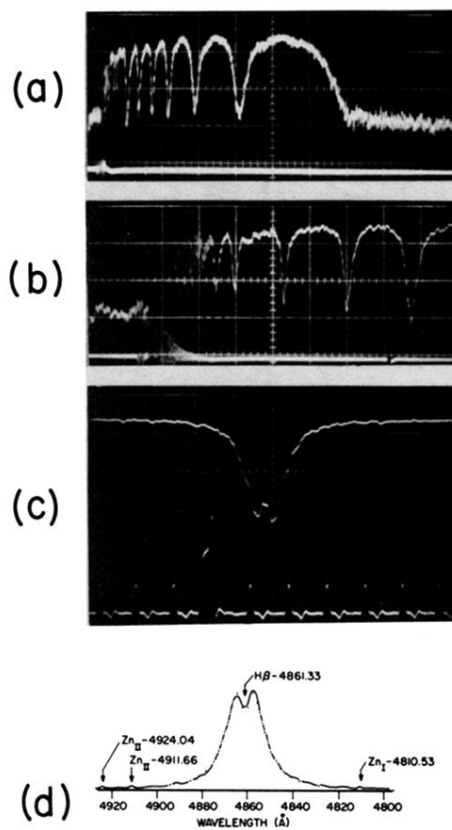


FIG. 2. Typical interferometer and spectrometer recordings. (a) $\lambda = 1.1523 \mu$ at $10 \mu\text{sec}/\text{div}$. (b) $\lambda = 1.1523 \mu$ at $2 \mu\text{sec}/\text{div}$. (c) An H_{β} line profile at $0.2 \mu\text{sec}/\text{div}$. The timing marks are from a 5-Mc/sec crystal-controlled pulser. The timing pulse, recorded on the lower traces, is derived from the firing of the discharge tube. (d) Comparison of an observed H_{β} profile [Fig. 2(c)] with its theoretical profile (dots). The narrow band at the bottom is the continuum intensity. $T = 2 \times 10^4 \text{ }^{\circ}\text{K}$. $N_e = 2.78 \times 10^{16} \text{ cm}^{-3}$.